

Generation of microwave radiation in planar spin-transfer devices

Ya. B. Bazaliy

*Instituut Lorentz, Leiden University, The Netherlands,
Department of Physics and Astronomy, University of South Carolina, Columbia, SC, and
Institute of Magnetism, National Academy of Science, Ukraine.*

(Dated: May, 2006)

Current induced precession states in spin-transfer devices are studied in the case of large easy plane anisotropy (present in most experimental setups). It is shown that the effective one-dimensional planar description provides a simple qualitative understanding of the emergence and evolution of such states. Switching boundaries are found analytically for the collinear device and the spin-flip transistor. The latter can generate microwave oscillations at zero external magnetic field without either special functional form of spin-transfer torque, or “field-like” terms, if Gilbert constant corresponds to the overdamped planar regime.

PACS numbers: 85.75.-d, 75.40.Gb, 72.25.Ba, 72.25.Mk

Spin-polarized currents are able to change the magnetic configuration of nanostructures through the spin-transfer effect proposed more than a decade ago [1, 2]. Intensive research is currently directed at understanding the basic physics of this non-equilibrium interaction and designing magnetic nanodevices with all-electric control.

Initial spin-transfer experiments emphasized the current induced switching between two static configurations [3]. Presently, the research focus is broadening to include the states with continuous magnetization precession powered by the energy of the current source [2, 4, 5]. Spin-transfer devices with precession states (PS) serve as nano-generators of microwave oscillations with remarkable properties, e.g. current tunable frequency and extremely narrow linewidth [6, 7, 8, 9]. A particular issue of technological importance is the search for systems supporting PS at zero magnetic field. Here several strategies are pursued: (i) engineering unusual angle dependence of spin-transfer torque [10, 11, 12], (ii) relying on the presence of the “field-like” component of the spin torque [13], (iii) choosing the “magnetic fan” geometry [14, 15, 16, 17].

PS are more difficult to describe than the fixed equilibria: the amplitude of precession can be large and non-linear effects are strong. As a result, information about them is often obtained from numeric simulations. Here

we study PS in planar devices [18] using the effective one-dimensional approximation [19, 20, 21] which is relevant for the majority of experimental setups. It is shown that planar approximation provides a very intuitive picture allowing to predict the emergence of precession and subsequent transformations between different types of PS. We show that PS in devices with in-plane spin polarization of the current can exist at zero magnetic field without the unusual properties (i),(ii) of the spin-transfer torque.

A conventional spin-transfer device with a fixed polarizer and a free layer (Fig. 1) is considered. The macrospin magnetization of the free layer $\mathbf{M} = M\mathbf{n}$ has a constant absolute value M and a direction given by a unit vector $\mathbf{n}(t)$. The LLG equation [2, 5] reads:

$$\dot{\mathbf{n}} = \frac{\gamma}{M} \left[-\frac{\delta E}{\delta \mathbf{n}} \times \mathbf{n} \right] + u(\mathbf{n})[\mathbf{n} \times \mathbf{s} \times \mathbf{n}] + \alpha[\mathbf{n} \times \dot{\mathbf{n}}]. \quad (1)$$

Here γ is the gyromagnetic ratio, $E(\mathbf{n})$ is the magnetic energy, α is the Gilbert damping constant, \mathbf{s} is the spin-polarizer unit vector. The spin transfer strength $u(\mathbf{n})$ is proportional to the electric current I [5, 20]. In general, it is a function of the angle between the polarizer and the free layer $u(\mathbf{n}) = f[(\mathbf{n} \cdot \mathbf{s})] I$, with the function $f[(\mathbf{n} \cdot \mathbf{s})]$ being material and device specific [22, 23, 24].

The LLG equation can be written in terms of the polar angles (θ, ϕ) of vector \mathbf{n} . Planar devices are characterized by the energy form $E = (K_{\perp}/2) \cos^2 \theta + E_r(\theta, \phi)$ with $K_{\perp} \gg |E_r|$. The first term provides the dominating easy plane anisotropy and ensures that the low energy motion happens close to the $\theta = \pi/2$ plane. The residual energy E_r has an arbitrary form. The smallness of $\delta\theta = \theta(t) - \pi/2$ allows to derive a single effective equation on the in-plane angle $\phi(t)$ by performing the expansion in small parameter $|E_r|/K_{\perp}$ [21]. For time-independent current and polarizer direction \mathbf{s} one obtains:

$$\frac{1}{\omega_{\perp}} \ddot{\phi} + \alpha_{eff} \dot{\phi} = -\frac{\gamma}{M} \frac{\partial E_{eff}}{\partial \phi}, \quad (2)$$

where $\omega_{\perp} = \gamma K_{\perp}/M$. General expressions for $\alpha_{eff}(\phi)$

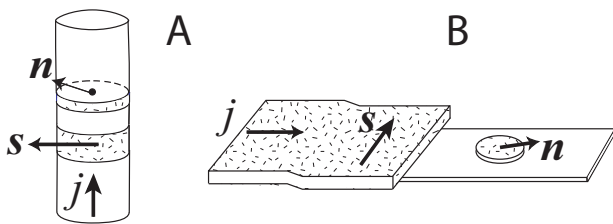


FIG. 1: Planar spin-transfer devices. Hashed parts of the devices are ferromagnetic, white parts are made from a non-magnetic metal.

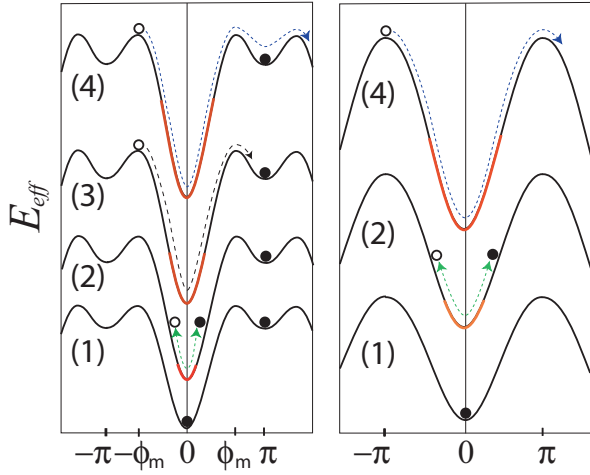


FIG. 2: (Color online) Evolution of effective energy profile and stable solutions with spin-transfer strength (graphs are shifted up as u becomes more negative) for a device with collinear polarizer. Left: low-field $0 < h < \tilde{\omega}_{\parallel}$ regime. Right: high-field $h > \tilde{\omega}_{\parallel}$ regime. Evolution stage (3) is missing in the high-field regime due to the absence of the second energy minimum. The red parts of the energy graphs mark the $\alpha_{eff} < 0$ regions. Filled and empty circle gives represent the effective particle.

and $E_{eff}(\phi)$ for arbitrary function $E_r(\theta, \phi)$ and polarizer direction \mathbf{s} are given in Ref. 21. In a special case frequently found in practice the polarizer \mathbf{s} is directed in the easy plane at the angle ϕ_s , and the residual energy satisfies $(\partial E_r / \partial \theta)_{\theta=\pi/2} = 0$, i.e. does not shift the energy minima away from the plane. We will also use the simplest form $f[(\mathbf{n} \cdot \mathbf{s})] = \text{const}$ for the spin transfer strength. A more realistic function can be employed if needed. With these assumptions [21]:

$$\alpha_{eff} = \alpha + \frac{2u \cos(\phi_s - \phi)}{\omega_{\perp}}, \quad (3)$$

$$E_{eff} = E_r(\pi/2, \phi) - \frac{Mu^2}{2\gamma\omega_{\perp}} \cos^2(\phi_s - \phi).$$

Equation (2) has the form of Newton's equation of motion for a particle in external potential $E_{eff}(\phi)$ with a variable viscous friction coefficient $\alpha_{eff}(\phi)$. The advantage of such a description is that the motion of the effective particle can be qualitatively understood by applying the usual energy conservation and dissipation arguments. In the absence of current, the effective friction is a positive constant, so after an initial transient motion the system always ends up in one of the minima of $E_r(\pi/2, \phi)$. When current is present, effective friction and energy are modified. Such a modification reflects the physical possibility of extracting energy from the current source, and leads to the emergence of the qualitatively new dynamic regime of persistent oscillations. These oscillations of ϕ correspond to the motion of \mathbf{n} along the highly elongated ($\delta\theta \ll 1$) closed orbits (see examples in Fig. 3, inset), i.e. constitute the limiting form of the precession states

[2, 5, 7, 25] in spin-transfer systems.

To illustrate the advantages of the effective particle description, consider a specific example of PS in the nanopillar experiment [7] where E_r is an easy axis anisotropy energy with magnetic field H directed along that axis, $E_r(\phi) = (K_{\parallel}/2) \sin^2 \phi - HM \cos \phi$. The polarizer \mathbf{s} is directed along the same axis with $\phi_s = 0$ (collinear polarizer). With the definitions $\omega_{\parallel} = \gamma K_a/M$, $h = \gamma H$, the effective energy becomes [21]

$$\frac{\gamma}{M} E_{eff} = \frac{\tilde{\omega}_{\parallel}(u)}{2} \sin^2 \phi - h \cos \phi, \quad (4)$$

with $\tilde{\omega}_{\parallel} = \omega_{\parallel} + u^2/\omega_{\perp}$. Effective energy profiles are shown in Fig. 2. For low fields, $|h| < \tilde{\omega}_{\parallel}(u)$, the minima at $\phi = 0, \pi$ are separated by maxima at $\pm\phi_m(h)$.

According to Eq. (3), the effective friction can become negative at $\phi = 0$ or $\phi = \pi$ at the critical value of spin-transfer strength $|u| = u_1 = \alpha\omega_{\perp}/2$. If this value is exceeded, the position of the system in the energy minimum becomes unstable. Indeed, the stability of any equilibrium in one dimension depends on whether it is a minimum or a maximum of E_{eff} and on the sign of α_{eff} at the equilibrium point. Out of four possible combinations, only an energy minimum with $\alpha_{eff} > 0$ is stable. A little above the threshold, α_{eff} is negative in a small vicinity of the minimum where the system is now characterized by negative dissipation. In this situation any small fluctuation away from the equilibrium initiates growing oscillations. As the oscillations amplitude exceeds the size of the $\alpha_{eff} < 0$ region, part of the cycle starts to happen with positive dissipation. Eventually the amplitude reaches a value at which the energy gain during the motion in the $\alpha_{eff} < 0$ region is exactly compensated by the energy loss in the $\alpha_{eff} > 0$ region: thus a stable cycle solution emerges (Fig. 2, profile (2)).

The requirement of zero total dissipation means that an integral over the oscillation period satisfies $\int \alpha_{eff}(\phi)(\dot{\phi})^2 dt = 0$. In typical collinear systems [25] Gilbert damping satisfies $\alpha \approx 0.01 \ll \sqrt{\omega_{\parallel}/\omega_{\perp}} \approx 0.1 \ll 1$, hence the oscillator (2),(4) operates in the lightly damped regime. In zeroth order approximation the friction term in (2) can be neglected, and a first integral $\dot{\phi}^2/(2\omega_{\perp}) + E_{eff} = E_0$ exists. Zero dissipation condition can be then approximated by

$$\int_{\phi_1}^{\phi_2} \alpha_{eff}(\phi) \sqrt{E_0 - E_{eff}(\phi)} d\phi = 0, \quad (5)$$

with $\phi_{1,2}(u)$ being the turning points of the effective particle trajectory, and $E_0 = E_{eff}(\phi_1) = E_{eff}(\phi_2)$. Since the integrand of (5) is a known function, the formula provides an expression for the precession amplitude.

Consider now the low positive field regime $0 < h < \tilde{\omega}_{\parallel}$. At $u = -u_1$ the parallel configuration becomes unstable and a cycle emerges near the $\phi = 0$ minimum. As u is made more negative, the oscillation amplitude grows

until eventually it reaches the point of energy maximum at $u = -u_2$. Equivalently, the effective particle starting at the energy maximum $-\phi_m$ is able to reach the other maximum at $+\phi_m$ (Fig. 2, left, (3)). Above this threshold the particle inevitably goes over the potential hill and falls into the $\phi = \pi$ minimum which remains stable since $\alpha_{eff}(\pi) > 0$ holds for negative u . In other words, the cycle solution with oscillations around $\phi = 0$ ceases to exist. At even more negative u the third threshold is reached when the effective particle can complete the full rotation starting from the energy maximum (Fig. 2, profile (4)). Below $u = -u_3$ a new PS with full rotation emerges. In the high-field regime $h > \tilde{\omega}_{||}$ the evolution of the precession cycle is similar (Fig. 2, right), but stage (3) is missing since there is no second minimum. The threshold $u = -u_2$ separates the finite oscillations regime and the full-rotation regime.

Thresholds u_i can be obtained analytically from (5) by substituting the critical turning points $\phi_{1,2}$ listed above:

$$u_2 = \alpha\omega_{\perp} \frac{h\phi_m + \omega_{||} \sin \phi_m}{\omega_{||}\phi_m + h \sin \phi_m} \quad (h < \omega_{||}), \quad (6)$$

$$u_2 = \alpha\omega_{\perp} \frac{h}{\omega_{||}} \quad (h > \omega_{||}), \quad (7)$$

$$u_3 = \alpha\omega_{\perp} \frac{h(\phi_m - \pi/2) + \omega_{||} \sin \phi_m}{\omega_{||}(\phi_m - \pi/2) + h \sin \phi_m} \quad (h < \omega_{||}). \quad (8)$$

The corresponding switching diagram is shown in Fig. 3 (cf. numerically obtained Fig. 12 in Ref. 25). It shows that different hysteresis patterns are possible depending on the trajectory in the parameter space.

PS in the low field regime was discussed analytically in an unpublished work [26]. However, since a conventional description with two polar angles was used, the calculations were much less transparent. Numeric studies of the PS were performed in Refs. [7, 25] after the experimental observation [7] of the current induced transition between two PS in the high field regime. They had shown that indeed the low-current precession state PS_1 has a finite amplitude of ϕ -oscillations, while the high-current state PS_2 exhibits full rotations of ϕ (Fig. 3, inset).

Next, we consider the cycle solutions in a device called a spin-flip transistor [18, 27]. It differs from the setup studied above in the polarizer direction, which is now perpendicular to the easy axis with $\phi_s = \pi/2$. No external magnetic field is applied. In this case [21]

$$\alpha_{eff} = \alpha + \frac{2u \sin \phi}{\omega_{\perp}}, \quad (9)$$

$$\frac{\gamma}{M} E_{eff} = \frac{\tilde{\omega}_{||}(u)}{2} \sin^2 \phi, \quad (10)$$

with $\tilde{\omega}_{||} = \omega_{||} - u^2/\omega_{\perp}$. As the spin-transfer strength grows, the behavior of the system changes qualitatively when $\tilde{\omega}_{||}$ or $\alpha_{eff}|_{\pm\pi/2}$ change signs at the thresholds $\bar{u}_1 = \pm\sqrt{\omega_{||}\omega_{\perp}}$ and $\bar{u}_2 = \pm\alpha\omega_{\perp}/2$. In accord with previous in-

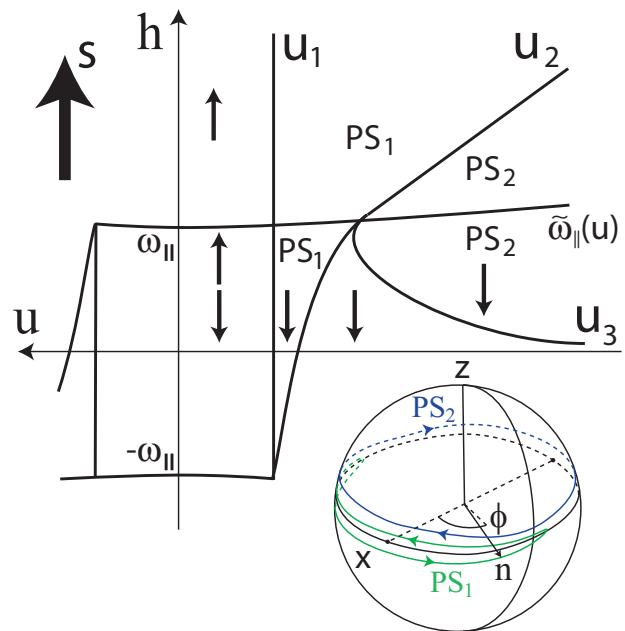


FIG. 3: (Color online) Switching diagram of a device with collinear polarizer. The u -axis direction is reversed for the purpose of comparison with Refs. 7, 25. The parts of the diagram not shown can be recovered by a 180-degree rotation of the picture. Stable directions in each region are given by small arrows, the precession states are marked as $PS_{1,2}$. The large arrow shows the polarizer direction. Inset: schematic trajectories of the $PS_{1,2}$ states on the unit sphere.

vestigations [16, 28] at $|u| > \bar{u}_1$ the $\phi = 0, \pi$ energy minima are destabilized and the parallel state $\phi = \text{sgn}[u]\phi_s$ becomes stable. Surprisingly, for $\alpha > \alpha_* = 2\sqrt{\omega_{||}/\omega_{\perp}}$ a window $\bar{u}_1 < u < \bar{u}_2$ of stability of antiparallel configuration, $\phi = -\text{sgn}[u]\phi_s$, opens (Fig. 4). As discussed in Ref. [21], the stabilization of the antiparallel state happens as the spin-transfer torque is increased in spite of the fact that this torque repels the system from that direction. At $u = \bar{u}_2$ the antiparallel state turns into a cycle (Fig. 4, low right panel) which we will study here. Above the \bar{u}_2 threshold the amplitude of oscillations grows until they reach the energy maximum at $u = \bar{u}_3$ and the cycle solution disappears. Although α is not small, \bar{u}_3 can still be determined from Eq. (5) because α_{eff} is small when u is close to u_2 . Calculating the integral in (5) with $\phi_{1,2} = -\pi, 0$ we get

$$\bar{u}_3 = \frac{2}{\pi} \alpha\omega_{\perp} \approx 1.27 \bar{u}_2. \quad (11)$$

The usage of approximations (5),(11) is legitimate for $\alpha \gtrsim 2\alpha_*$ where $\alpha_{eff}(\bar{u}_3) \ll \sqrt{\tilde{\omega}_{||}(\bar{u}_3)}/\omega_{\perp}$ holds. For smaller values of α numeric calculations are required. They show the existence of a stable cycle down to $\alpha = 0.8\alpha_*$ where the stabilization of the antiparallel state is impossible. For $\alpha \ll \alpha_*$ and $u \gtrsim \bar{u}_1$ the strong negative dissipation regime is realized, $|\alpha_{eff}| \gg \sqrt{\tilde{\omega}_{||}/\omega_{\perp}}$. Numeric results show that the amplitude of the oscillations

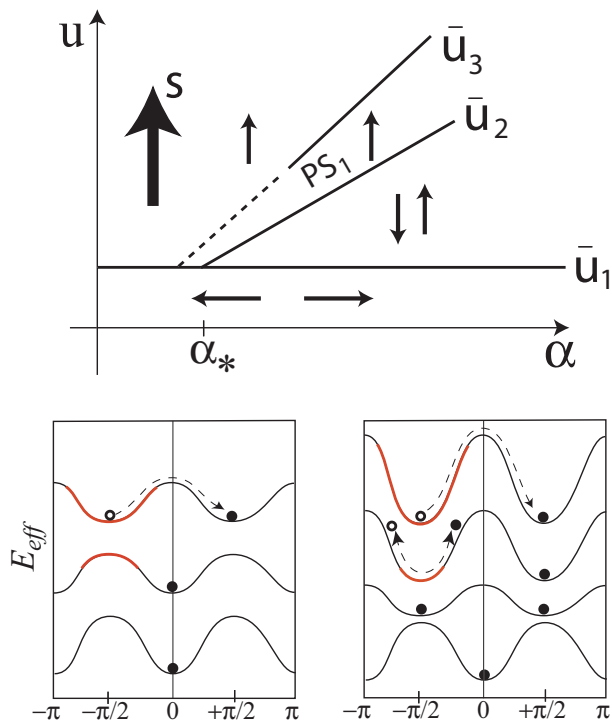


FIG. 4: (Color online) Switching diagram of a spin-flip transistor. The $u < 0$ part of the diagram can be obtained by reflection with respect to the horizontal axis. In each region stable directions are given by small arrows, precession state is marked by PS_1 . The large arrow shows the polarizer direction. Threshold $\bar{u}_3(\alpha)$ is sketched as a dashed line where approximation (11) is not valid. Lower panels: the evolution of effective energy and trajectories (graphs are shifted up with growing u) at $\alpha \ll \alpha_*$ (left) and $\alpha > \alpha_*$ (right). The red part of the energy graph marks the $\alpha_{eff} < 0$ region. Effective particle is shown by filled and empty circles.

induced by negative dissipation is so big that the effective particle always reaches the energy maximum and drops into the stable parallel state (Fig 4, low left panel). We conclude that the line $\bar{u}_3(\alpha)$ crosses the $u = \bar{u}_1$ line at some point and terminates there.

As for the full-rotation PS, one can show analytically that it does not exist in the small dissipation limit at $\alpha \gtrsim 2\alpha_*$. Numerical simulations do not find it in the $\alpha < \alpha_*$, $u > \bar{u}_1$ regime either.

In conclusion, we have shown that the planar effective description can be very useful for studying precession solutions in the spin transfer systems. It was already used to describe the “magnetic fan” device with current spin polarization perpendicular to the easy plane [20]. Here the switching diagrams were obtained for the spin polarizers directed collinearly and perpendicular to the easy direction within the plane. In collinear case we found analytic formulas for the earlier numeric results, while the study of precession solutions in the perpendicular case (spin-flip transistor) at large damping is new. The latter shows the possibility of generating microwave oscil-

lations in the absence of external magnetic field without the need to engineer special angle dependence of the spin-transfer torque or “field-like” terms. The inequality $\alpha > 2\sqrt{\omega_{||}/\omega_{\perp}}$ required for the existence of such oscillations can be satisfied by either reducing the in-plane anisotropy, or increasing α due to spin-pumping effect [29]. Most importantly, the effective planar description allows for qualitative understanding of the precession cycles and makes it easy to predict their emergence, subsequent evolution, and transitions between different precession cycle types. E.g., in the systems with one region of negative effective dissipation, such as considered here, it shows that no more than two precession states, one with finite oscillations and another with full rotations, can exist. Numerical approaches, if needed, are then based on a firm qualitative foundation. In addition, numerical calculations in one dimension are easier than in the conventional description with two polar angles.

The author thanks G. E. W. Bauer and M. D. Stiles for discussion. Research at Leiden University was supported by the Dutch Science Foundation NWO/FOM. Part of this work was performed at Aspen Center for Physics.

-
- [1] L. Berger, *J. Appl. Phys.*, **49**, 2160 (1978); *Phys. Rev. B* **33**, 1572 (1986); *J. Appl. Phys.* **63**, 1663 (1988).
 - [2] J. Slonczewski, *J. Magn. Magn. Mater.* **159**, L1 (1996).
 - [3] J. A. Katine *et al.*, *Phys. Rev. Lett.*, **84**, 3149 (2000).
 - [4] J. Z. Sun, *Phys. Rev. B* **62**, 570 (2000).
 - [5] Ya. B. Bazaliy *et al.*, arXiv:cond-mat/0009034 (2000); *Phys. Rev. B*, **69**, 094421 (2004).
 - [6] M. Tsoi *et al.*, *Nature*, **406**, 46 (2000).
 - [7] S. I. Kiselev *et al.*, *Nature*, **425**, 380 (2003).
 - [8] S. Kaka *et al.*, *Nature* **437**, 389 (2005);
 - [9] M. R. Pufall *et al.*, *Phys. Rev. Lett.* **97**, 087206 (2006);
 - [10] J. Manschot *et al.*, *Appl. Phys. Lett.* **85**, 3250 (2004).
 - [11] M. Gmitra *et al.*, *Phys. Rev. Lett.*, **96**, 207205 (2006).
 - [12] O. Boulle *et al.*, *Nature Physics*, May 2007.
 - [13] T. Devolder *et al.*, *J. Appl. Phys.*, **101**, 063916 (2007)
 - [14] A. D. Kent *et al.*, *Appl. Phys. Lett.*, **84**, 3897 (2004)
 - [15] K. J. Lee *et al.*, *Appl. Phys. Lett.*, **86**, 022505 (2005).
 - [16] X. Wang *et al.*, *Phys. Rev. B*, **73**, 054436 (2006).
 - [17] D. Houssameddine *et al.*, *Nature Materials*, April 2007.
 - [18] A. Brataas *et al.*, *Phys. Rep.*, **427**, 157 (2006).
 - [19] C. Garcia-Cervera *et al.*, *J. Appl. Phys.*, **90**, 370 (2001).
 - [20] Ya. B. Bazaliy *et al.*, arXiv:0705.0406v1 (2007), to be published in *J. Nanoscience and Nanotechnology*.
 - [21] Ya. B. Bazaliy, arXiv:0705.0508 (2007).
 - [22] J. C. Slonczewski, *JMMM*, **247**, 324 (2002).
 - [23] A. A. Kovalev *et al.*, *Phys. Rev. B*, **66**, 224424 (2002)
 - [24] J. Xiao *et al.*, *Phys. Rev. B*, **70**, 172405 (2004).
 - [25] J. Xiao *et al.*, *Phys. Rev. B*, **72**, 014446 (2005)
 - [26] T. Valet, unpublished preprint (2004).
 - [27] A. Brataas *et al.*, *Phys. Rev. Lett.* **84**, 2481 (2000);
 - [28] H. Morise *et al.*, *Phys. Rev. B*, **71**, 014439 (2005).
 - [29] Ya. Tserkovnyak *et al.*, *Rev. Mod. Phys.*, **77**, 1375 (2005).